NANO LETTERS

pubs.acs.org/NanoLett

Growth Mechanism of Self-Catalyzed Group III−V Nanowires

Bernhard Mandl,*,†,‡ Julian Stangl,‡ Emelie Hilner,§ Alexei A. Zakharov,∥ Karla Hillerich,† Anil W. Dey,⊥ Lars Samuelson,† Günther Bauer,‡ Knut Deppert,† and Anders Mikkelsen§

†Solid State Physics, Lund University, S-22 100 Lund, Sweden, ‡Institute of Solid State- and Semiconductor Physics, Johannes Kepler University Linz, A-4040 Linz, Austria, §Synchrotron Radiation Research, Lund University, S-22 100 Lund, Sweden, ∥MAXLab, Lund University, S-22 100 Lund, Sweden, and ⊥Department of Electrical and Information Technology, Lund University, S-22 100 Lund, Sweden

ABSTRACT Group III−V nanowires offer the exciting possibility of epitaxial growth on a wide variety of substrates, most importantly silicon. To ensure compatibility with Si technology, catalyst-free growth schemes are of particular relevance, to avoid impurities from the catalysts. While this type of growth is well-documented and some aspects are described, no detailed understanding of the nucleation and the growth mechanism has been developed. By combining a series of growth experiments using metal−organic vapor phase epitaxy, as well as detailed in situ surface imaging and spectroscopy, we gain deeper insight into nucleation and growth of self-seeded III−V nanowires. By this mechanism most work available in literature concerning this field can be described.

KEYWORDS Nanowire, nanowire nucleation mechanism, nanowire growth mechanism, surface imaging and spectroscopy

One of the most intriguing features of semiconductor nanowires is the ability to realize epitaxial growth of material combinations not realized in bulk or layer growth.[1−3] Of particular interest is the growth of group III−V semiconductors on Si substrates, exploiting the mature Si technology, the availability of large substrates in combination with the superior optoelectronic and electronic properties of III−V compounds. Metal seed particles are widely used for nanowire growth, preferentially Au nanoparticles.[4−6] For the combination with Si technology, this is problematic due to Au forming deep level traps in Si. Therefore, several growth schemes avoiding foreign metal seed particles have been developed. A variety of mechanisms of catalyst-free growth have been suggested,[7−14] but surprisingly little systematic work has been performed to establish these mechanisms firmly, and more importantly, to determine the actual relevant one for wire nucleation. In the following we present a series of experiments on the growth of InAs nanowires as a model system to clarify this point for III−V semiconductors. The InAs material system in itself is extremely relevant for high-speed electronics,[15,16] and it has turned out to be difficult to establish the precise growth mechanism for this particular system. We show that for the majority of experiments, wire nucleation and growth are explained in a unified way by group-III-seeded growth, despite rather different postgrowth observations.

We first briefly summarize the relevant general categories of nanowire growth mechanisms which have been proposed. These can be grouped into two different basic mechanisms each with two subcategories. One is based on the suppression of crystal growth in two directions to create one-dimensional structures, as is the case for selective area epitaxy (SAE) and oxide-assisted growth (OAG). SAE employs a mask layer with well-defined openings, out of which wires grow in a layer-by-layer mode (Figure 1a). The fact that growth continues one-dimensionally also above the mask layer, in contrast to lateral overgrowth, is attributed to the formation of slowly growing side facets with a low surface energy.[7] For this kind of growth, no seed particle is used. OAG is based on the use of the semiconductor and one of its oxides. During growth, phase separation occurs, leading to a core of the semiconductor material, which is simultaneously covered by a passivating shell of its oxide (Figure 1b), suppressing lateral growth.[10]

The second group of 1D growth mechanisms is based on a significant local increase of growth velocity in one direction, in many cases caused by a particle at the wire top.[17] For these particle-assisted growth (PAG) schemes, we may distinguish between seed particles containing elements constituting the wire (homoparticle assisted growth, Figure 1c), and seed particles of a different material (heteroparticle assisted growth, Figure 1d). In both cases, supersaturation of the growth system leads to material crystallizing rapidly at the particle/crystal interface. The seed particle can be either liquid (vapor−liquid−solid growth, VLS) or solid (vapor−solid−solid growth, VSS).

In the following we will compare our experimental results with the predictions arising from the different growth models and show that catalyst-free III−V nanowire growth is actually widely based on a group III homoparticle-assisted VLS growth. We will first rule out the growth modes based on suppression of growth on the side facets and later on test

* To whom correspondence should be addressed, Bernhard.Mandl@jku.at.
Received for review: 06/29/2010
Published on Web: 10/07/2010

DOI: 10.1021/nl1022699 | *Nano Lett.* **2010,** *10,* 4443–4449

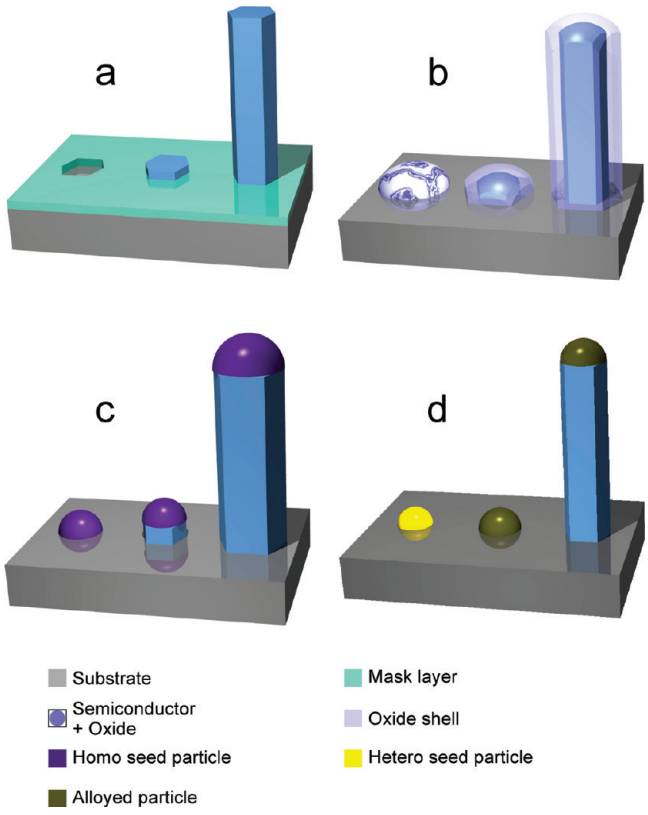

FIGURE 1. Schematic representation of four basic nanowire growth mechanisms: (a) Selective area epitaxy. An epitaxial layer nucleates in openings of a mask layer and continuously grows in height, its lateral growth is restricted by low-energy facets. (b) Oxide-assisted growth. The semiconductor and its oxide are adsorbed on the surface, creating nucleation centers which separate into a semiconductor core and a passivating oxide shell. (c) Homoparticle growth. A seed particle is formed consisting of one or all elements used for wire growth. During growth both length and diameter increase as the seed particle size is variable. (d) Heteroparticle growth. A seed particle (typically Au) is deposited prior to growth. During heating to growth temperature the seed particle alloys with the substrate and/or material from the gas phase. Particle size during growth is nearly constant.

the validity of PAG using a combination of growth studies and surface microscopy. After identifying the growth mechanism for nanowire growth, we study the mechanism responsible for particle formation leading to nanowire nucleation.

For our work, the growth of InAs nanowires was used as a model system to understand the underlying growth mechanism for III−V nanowires. The wires are grown in a temperature range between 520 and 660 °C, if nothing else is stated, a growth temperature of 580 °C is used. We studied the growth of InAs nanowires on different substrates (namely, InAs, InP, GaAs, GaP, and Si, if nothing else is stated InAs(111)B is used) covered by a thin (≈13 Å measured by an oscillating quartz crystal inside the evaporator) SiO_x ($x \approx 1$) layer, produced by thermal sublimation; for a SiO_x layer with a thickness larger than ≈5 nm no wire growth was found. The wires typically grow epitaxially along the [111]B direction of the substrate and show a hexagonal cross

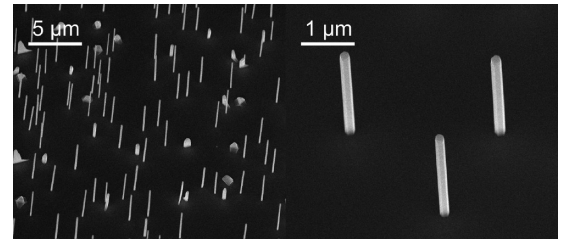

FIGURE 2. Scanning electron micrograph of nanowires: left, typical morphology of InAs nanowires and islands grown on an InAs(111)B substrate covered with ≈13 Å SiO_x for 8 min; right, close up image of InAs nanowires on an InAs(111)B substrate with a ≈ 13 Å SiO_x layer, showing the shape of the wires, samples are part of the data shown in Figure 3. The samples are tilted by 30°.

section truncated by {110} side facets. A typical nanowire sample imaged by scanning electron microscopy (SEM) is shown in Figure 2. Metal−organic vapor phase epitaxy (MOVPE) was used in two different systems (EPIQUIP VP502-RP and AIXTRON AIX 200/4) to compare the stability of growth with respect to the growth equipment. As carrier gas H_2 was used at a pressure of 100 mbar at a flow rate of 6000 mL/min (Epiquip VP502-RP) or 13000 mL/min (Aixtron AIX 200/4). As precursors we used trimethylindium (TMI) and AsH_3 at molar fractions of 3.1×10^{-6} and 8.3×10^{-4}, respectively. The substrates were heated under H_2 atmosphere to growth temperature between 520 and 660 °C, at which the precursors were activated simultaneously. No particles were deposited prior to nanowire growth. Growth was terminated by turning off the TMI flow, and the samples were cooled under an arsine flow to a temperature of 300 °C. At temperatures lower than 200 °C the samples were removed from the growth reactor. We note that in a MOVPE system there is always a background pressure of the group V elements due to evaporation of material which was deposited at the reactor side walls.

For studies on the wire nucleation on the substrates, measurements were performed with an Elmitec spectroscopic photoemission and low-energy electron microscope (SPELEEM) III[18] connected to the soft X-ray beamline I311 at MAX-Lab in Lund.[19] All SPELEEM imaging and annealing was performed in ultrahigh vacuum at a base pressure <1 $\times 10^{-10}$ mbar. The temperature was calibrated using a pyrometer and a thermocouple on the sample holder. Substrates investigated consisted of InAs(111)B substrates similar to the ones used for growth experiments. Both InAs(111)B substrates with and without SiO_x layers were investigated. The SiO_x layers were deposited in the same deposition system and following the same procedure as for the samples used for growth of nanowires. Samples where only one-half was covered with SiO_x were fabricated by covering half of the sample surface by the sample holder during SiO_x evaporation.

By careful evaluation of the lengths and diameters of at least 52 wires on each sample (using SEM images), the influence of growth duration and growth temperature on nanowire length and diameter was found. For sample

DOI: 10.1021/nl1022699 | *Nano Lett.* **2010,** *10,* 4443–4449

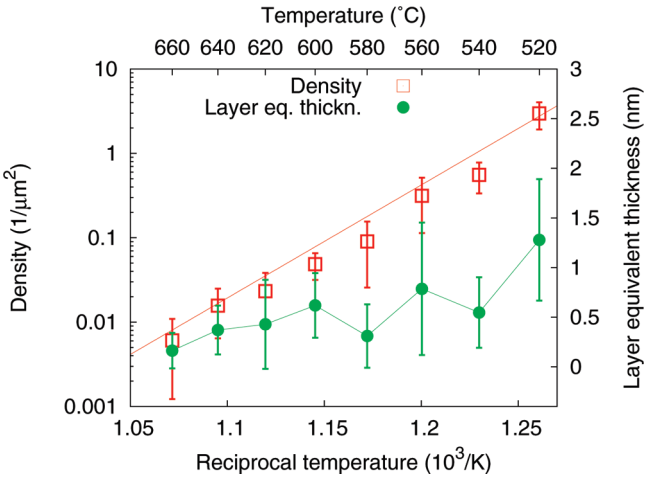

FIGURE 3. Influence of growth temperature: Density of nucleated structures and total volume of grown material represented as the equivalent thickness of a 2D layer (in both cases wires and dots between the wires are evaluated). For the density a minimum of five SEM images showing between 10 and 1000 structures per image are used. The layer equivalent thickness is the product of mean structure volume and mean structure density. Error bars represent the statistical spread of the measured values.

characterization we used several SEM instruments, namely, JEOL 6400F, FEI NanoLab 600, and a Leo Supra 35. Changing the growth time from 10 to 7200 s leads to an increase of not only the wire length (10 s, $0.101 \pm 0.035\,\mu$m; 7200 s, $26.14 \pm 2.13\,\mu$m) but also the diameter (10 s, 70 ± 22 nm; 7200 s, 514 ± 55 nm). Even though the diameter increases, no tapering of the wires can be found.

The observed growth in diameter and length directly rules out the OAG mechanism. Because the OAG growth mechanism relies on solid oxide sidewalls to establish 1D growth, this growth mode is immediately ruled out based on the observed diameter growth. Since no heteroparticles are used to catalyze growth in our case, only SAG and homo-PAG remain as possible growth mechanisms.

The basic assumption of the SAE mechanism is the presence of a mask layer which hinders growth except in specific openings; in the present case the SiO_x film might form such a mask layer. As described above, for SAE 1D growth is created by very slow growing low surface energy side facets. In this growth mechanism no seed particle is used. Therefore, to test the validity of SAE, we need to evaluate the behavior of the SiO_x layer at growth temperatures and compare this with the density and regularity of the nanowires.

To establish the density and regularity of growth nucleation, we grew samples in the temperature range between 520 and 660 °C. In the Arrhenius plot of the structure density the linear behavior (Figure 3) indicates an activation energy based process. The temperature has no substantial influence on the total amount of deposited material; it has been shown that the growth limiting precursor at these temperatures is completely cracked[20] as well as there is no considerable desorption of adsorbed material. However, a considerable decrease in density of all nucleated structures on the surface with increasing temperature is observed. Explaining the density change with temperature is difficult if SAE growth is assumed, as this would indicate also a radical decrease in the density of openings in the film with temperature. This volatility of the SiO_x film is in contradiction to the fundamental assumption of SAE mechanism of a stable mask necessary for stable nanowire growth.

To clarify the oxide behavior, we evaluated the temperature stability of the SiO_x layer by direct annealing studies of this layer on InAs(111)B in a SPELEEM, which reveals any changes in thickness or composition of the film with monolayer precision. Prior to annealing above 500 °C, no openings or major irregularities are observed in the film. As shown in panels a–c of Figure 4, annealing at 600 °C for 10 min leads to a formation of a multitude of openings with sizes ranging from <100 nm up to several micrometers in the SiO_x layer. If SAE growth is assumed, the wire diameter distribution should be directly correlated to the size of the openings in the film. For wires we find a diameter distribution of 70 ± 22 nm for 10 s growth time, a comparatively narrow size distribution, in direct contrast to the SPELEEM observations.

Also, if the number of nanowires depends directly on the number of openings in the mask on the substrate, the study of the influence of the growth temperature leads to the conclusion that increasing growth temperature results in a decrease in the number of openings in the film. This is again *inconsistent* with the SPELEEM studies where no such temperature dependence of the number of openings could be observed.

Therefore, we investigated whether particle-assisted growth using self-forming particles is consistent with the temperature behavior. Increasing the temperature has the following consequences: (i) increase of precursor decomposition and thus material deposition; (ii) increased desorption of adatoms from the substrate surface (not relevant in the T range we used); (iii) increased surface diffusion length. All of theses processes are activation energy dependent.[21] From the results presented in Figure 3, we can clearly see that on one hand the density of structures decreases with increasing temperature, while on the other hand no considerable change in the deposited volume is found. The growth-limiting precursor is fully decomposed in the used temperature range.[20] The decrease in wire density combined with no dramatic change in the deposited volume clearly shows that the increase in surface diffusion and not desorption is responsible for the change in the structure density. This means that with increasing temperature the adsorbed atoms can diffuse over a longer distance and fewer seed particles form. The dependence of diffusion length on temperature is given by an activation energy,[21] as is seen in Figure 3. Particle-assisted growth is perfectly consistent with the *decrease* in the number of nucleated structures with increasing temperature and, hence, is a strong candidate for

DOI: 10.1021/nl1022699 | *Nano Lett.* **2010,** *10,* 4443–4449

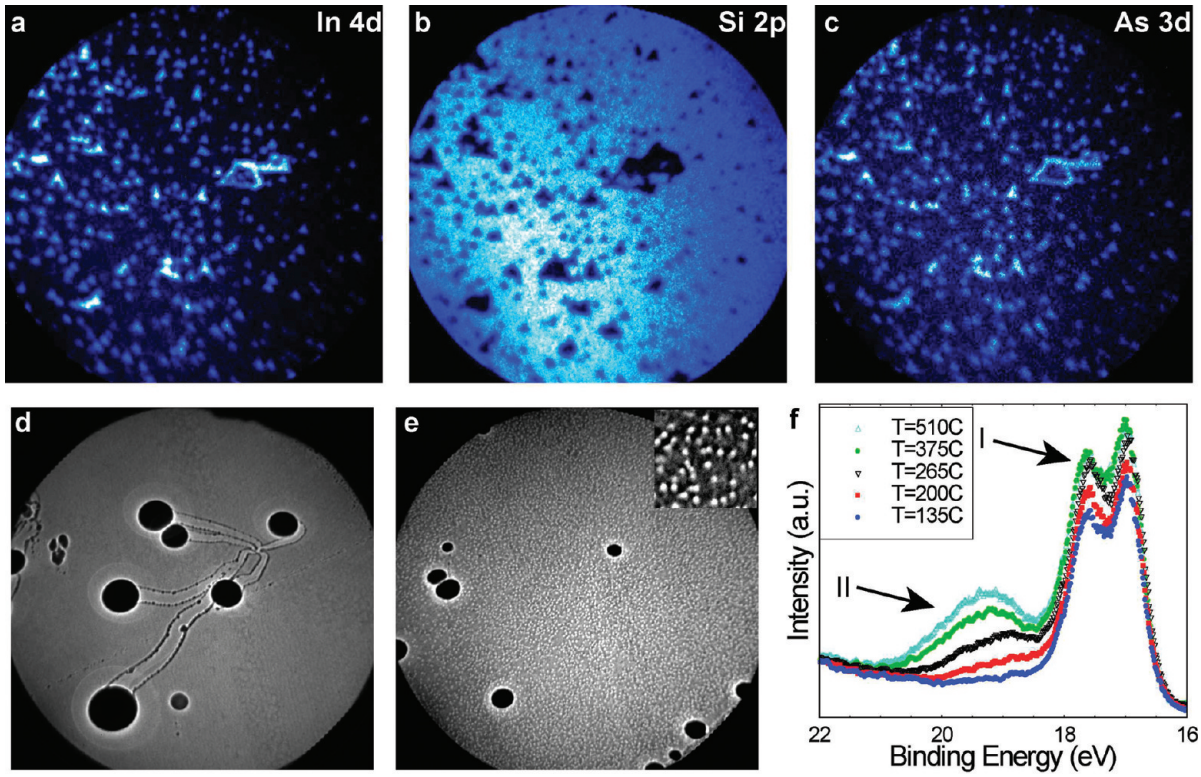

FIGURE 4. SPELEEM investigation of the InAs/SiO_x system. (a−c) 25 × 25 μ m^2 SPELEEM images of the SiO_x layer taken after annealing at 600 °C for 10 min. The image was recorded using photoelectrons of the Si 2p and In 4d and As 3d core levels, respectively, using a photon energy of 130 eV. Images were recorded at T = 520 °C. (d, e) 50 × 50 μm^2 low-energy electron microscopy (LEEM) images of the clean and SiO_x covered InAs(111)B surface after flashing the sample up to 600 °C for less than a minute. Droplets have formed both on clean InAs and on SiO_x covered InAs. On the SiO_x covered surface also small bright In islands have formed, which can be seen in the 3 × 3 μm^2 inset in (e). The islands are around 100 nm or less. If the droplets move, they leave traces behind (seen in (d) but not in (e)), which shows that droplets only move on the clean surface but not on the SiO_x covered surface (a LEEM movie recorded during annealing of the SiO_x covered surface is provided in Supplementary Movie 1 in the Supporting Information). The In nature of both the large droplets and the small white dots can be directly confirmed by μ-X-ray photoelectron spectroscopy (μ-XPS). (f) In 4d XPS spectra recorded on the SiO_x as a function of temperature. The peak marked I originates from In binding to As. As the temperature is raised, a new peak appears at 19 eV (peak II), the peak disappears again upon cooling down as can be seen from the temperature series in the graph. The position of the peak indicates that this is In binding to the oxide and not metallic In which would appear on the other side of peak I in binding energy.

the growth mechanism in our case. Assuming the possibility that the wires grow by particle-assisted growth raises the question which material forms the seed particle. We have used different substrate materials (InAs, InP, GaAs, and GaP, all with (111)B surface orientation, as well as Si(111)) for InAs nanowire growth,[22] InAs nanowires grown on a GaP(111)B and a Si(111) substrate are shown in Figure 5. Since the catalytic particle has to develop during growth, it has to be a combination of the elements present in the different substrates, oxide layer, and/or the gas phase. The only elements obviously present on the surface in all cases are In and As from the gas phase and Si and O from the SiO_x layer. For growth on III−V substrates, the only supply of Si is the ultrathin SiO_x layer, which would not be able to supply enough material during the entire wire growth time to enable the increase in nanowire diameter, which is accompanied by an increase of the particle volume by a factor of 250 when comparing wires grown for 10 s to those grown for 7200 s. So we concentrate on In and As. As has a sublimation temperature of ≈614 °C and does not remain on the surface at the higher growth temperatures (up to 660 °C) in this work; hence As will not form a catalytic particle. Thus the natural candidate for a particle is In, which might form a liquid droplet for the range of growth conditions investigated.

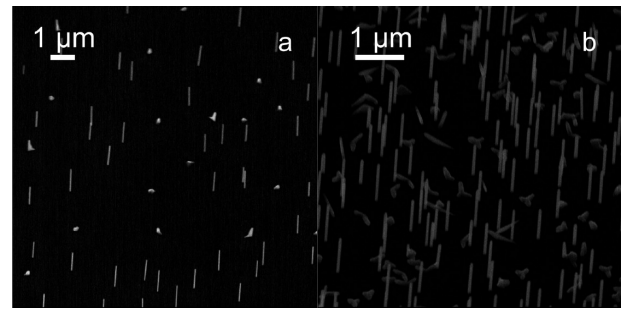

FIGURE 5. Growth of InAs nanowires on (a) GaP(111)B and (b) Si(111). The samples are covered by ≈1.3 and ≈0.9 nm thick SiO_x layers for the GaP and Si substrates, respectively. The samples are tilted by 22.4° in the images.

To test this assumption, we investigated the influence of a particular precursor on the stability of growth. After the "standard" growth conditions are applied for 120 s, an

DOI: 10.1021/nl1022699 | *Nano Lett.* **2010,** *10,* 4443–4449

interruption step follows for 30 s, during which TMI or AsH_3 or both flows are stopped. Hence the nanowires are effectively annealed under a flow of either the remaining precursor and H_2 or H_2 alone. After this step the growth conditions are restored by activating all precursors, and growth is continued for additional 120 s. Nanowires grown for 240 s without interruption serve as a reference. Wires grown with annealing under TMI + H_2 (3.43 ± 0.48 μm) have approximately the same length as those of the reference sample (3.39 ± 0.33 μm), while in the other cases the wires are significantly shorter ($AsH_3 + H_2$, 2.64 ± 0.16 μm; H_2, 2.67 ± 0.36 μm). The length does follow a power dependency ($l(t) \sim t^{\alpha}$ with $0.5 < \alpha < 0.6$);[23] double the growth time does not give double the wire length. Our interpretation is the following: during standard growth conditions, a liquid In droplet is formed, catalyzing wire growth. The supply for this droplet is from the TMI in the gas phase, so its size can vary during growth. When TMI is switched off, but AsH_3 is available, this drop crystallizes to InAs. When TMI is switched on again, a new In droplet may form, but not preferentially at the tip of a wire, so wire growth is actually terminated by the growth interruption. On the other hand, if the AsH_3 flow is interrupted, but TMI provided all the time, the In particle "survives" the growth interruption and growth can continue. From this experiment we are confident that In plays *the* central role in nanowire growth and forms the liquid droplet at the top of the wires inducing growth. It remains, however, a fact that without the SiO_x layer, wire growth cannot be achieved.

To understand in more detail the role of the SiO_x layer, which is essential for initial wire nucleation, we performed further studies at growth temperatures using SPELEEM. We investigated InAs(111)B with and without the SiO_x layer and samples where half the sample was covered by SiO_x to compare exactly identical experimental conditions. Due to the ultrahigh vacuum conditions of the SPELEEM, the temperature has to be increased above 550 °C to decompose the native oxides and to release free In on the surfaces. As there was no external In source available, this process was used as an In source for the SPELEEM experiments. On the clean surface, significant release of In, even after removal of the epi-ready oxide, occurs due to decomposition of InAs. As a result, In droplets of the size of a micrometer form within 10 s at around 520 °C. These droplets move around on the surfaces at a speed of several nanometers per second (group III droplet motion has been observed for other III−V surfaces recently[24,25]). In contrast, on SiO_x covered InAs, a high density of small droplets with homogeneous diameters of <100 nm appears after annealing above 550 °C. For samples where only half was covered with SiO_x, larger droplets also form on the SiO_x areas, due to the large amount of free In available; however in contrast to the clean surface the droplets are immobile. In addition, as shown in Figure 4f, a new peak appears in the In 4d photoemission spectra from the surface as the temperature is increased, coinciding with the appearance of the small dots. We interpret this as In being released from the InAs substrate during temperature increase (As evaporates). Remarkably, both the additional In 4d peak and the droplets disappear again upon cooling down the InAs substrate. This is interpreted as "free" In moving from the SiO_x surface to the interface between the SiO_x and the InAs. The movement can occur at rather low temperatures and is very fast indicating that the SiO_x film is transparent to diffusion of In. Energy-dependent measurements show that the "free" In does not disappear, but the signal is attenuated by the SiO_x layer on top of the InAs substrate. We find that In can diffuse through the SiO_x layer even before it has cracked up; however, we cannot exclude that the In primarily diffuses at certain specific points in the oxide.

We can now establish that the main role of the SiO_x film is to immobilize the In in well-defined areas on the surface and to change the size and density distribution from few very large to many small droplets. To investigate the SiO_x stability and fundamental behavior, ultrahigh vacuum studies using SPELEEM can be very relevant. In MOVPE the addition of growth species is not likely to change the general properties of the oxide, while the presence of the hydrogen carrier gas is likely to decrease the decomposition temperature of the oxide, also there should not be any difference for the mobility of the In droplets due to the different atmospheres in the SPELEEM and the MOVPE. From these small, well-defined In droplets the nanowires can now nucleate and grow. So far only the suitability of a SiO_x layer with $x \approx 1$ was demonstrated. To clarify whether its O concentration is crucial for wire nucleation, we also tested a SiO_2 layer on Si: an about 30 nm thick SiO_2 layer was produced by thermal oxidation, into it openings were etched by defining their positions in a resist layer using electron beam lithography (EBL), followed by a subsequent etching step using 4.6 mol % HF in H_2O solution. Prior to wire growth, the samples were annealed at 625 °C for 10 min[26] following the procedure proposed in ref 12. The wire growth was performed for 4 min using a molar fraction of 4.4×10^{-6} and 1.1×10^{-3} in 6000 mL/min H_2 for TMI and AsH_3, respectively; the growth temperature was 550 °C. As in the case of the SiO_x layer, highly uniform wires nucleate in the openings. Thus also here wire growth can clearly not be attributed to the SAE mechanism, as the wire diameters are smaller than the openings in the SiO_2 mask layer, as shown in Figure 6. This demonstrates that the O content in the layer does not influence the wire nucleation.

A remaining question is why no In droplets are observed at the top of the nanowires after growth. The most likely scenario is that the droplet simply crystallizes into an InAs tip on top of the InAs wire, since during cooling the AsH_3 flow in the reactor is still maintained in order to avoid wire decomposition. Depending on the growth temperature, in our MOVPE reactor it takes between 5 and 15 min to cool the samples from growth temperature to 400 °C, the temperature below which

DOI: 10.1021/nl1022699 | *Nano Lett.* **2010,** *10,* 4443–4449

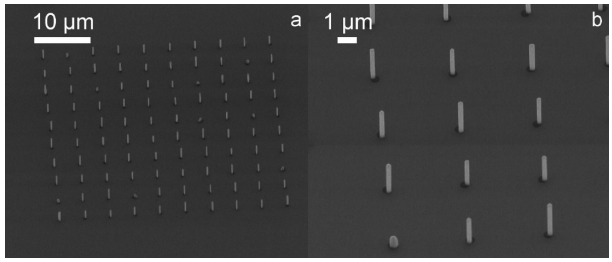

FIGURE 6. SEM images of InAs nanowires on a Si(111) substrate using a SiO_2 mask: (a) image of the whole pattern; (b) image showing a part of the EBL pattern, here it can clearly be seen that the openings are larger than the wires. The sample is tilted by 45°.

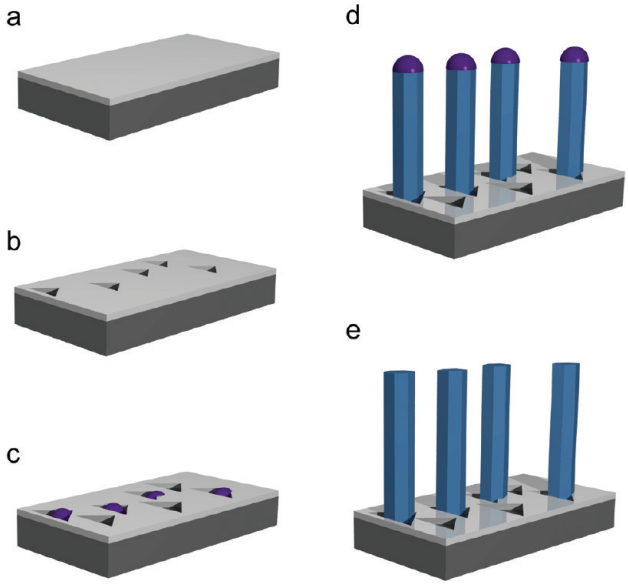

FIGURE 7. Schematic illustration of the growth mechanism: (a) layer before growth; (b) layer during heating of the sample, creation of openings; (c) formation of In droplets directly after activating the source material; (d) growth of the nanowires under the In droplets; (e) solidification of the droplets during cooling of the sample.

no further AsH_3 cracking occurs[27] and InAs growth therefore stops. This time is much longer than the time needed to consume the In droplet at the wire tip. Even for the thickest wires in our study and the lowest InAs growth rates, the In on the wire tip forms InAs within 1 min. Hence no In droplet is expected to be observed ex situ after growth.

Our experiments show that InAs nanowires are grown in a VLS mechanism using a liquid In droplet. The presence of the oxide layer is important to immobilize In droplets on the surface restricting the particle size and by that making nanowire nucleation possible. In conclusion, based on the experiments presented above, we see that nanowires grow in the sequence, as illustrated in Figure 7: (i) In the deposited SiO_x openings form during heating the substrate to growth temperature. (ii) When the TMI precursor is activated, the In atoms adsorbed on the surface diffuse into immobile In droplets formed in the openings of the SiO_x layer. The density of the In droplets depends on temperature as the temperature dependence of the diffusion length of the In ad atoms results in a ripening similar to what has been observed for In droplets on GaAs previously.[28] (iii) At the interface between these In particles and the substrate underneath, nanowire growth is initiated by enhancing the growth rate in one direction in a VLS mechanism.[17] (iv) After deactivation of the TMI supply, the droplet forms InAs with AsH_3 from the gas phase.

Parts of the here proposed mechanism have already been reported in literature, especially the use of group III particles for nanowire growth, but little is known so far on how these particles are created and how substrate material and growth conditions influence the particle formation. Many groups use such a layer, and understanding the function of this layer enables us now to describe a broad range of catalyst-free nanowire growth modes by one mechanism. Comparable growth results for In−V and Ga−V nanowires have been published previously, and various mechanisms have been proposed for InAs,[8,9,11,12,29−32] InP,[13,33−35] and GaAs[7,36−41] nanowires. In general the results can be discriminated in two regimes, characterized by the growth temperature. The high growth temperature regime (500−700 °C) is the regime with which our work deals. Comparing our growth parameters with those published previously for InAs nanowires, one finds only marginal differences. In all cases, either a covered substrate (with silicon oxide or nitride layers, or an organic layer), sometimes with intentionally etched openings in this layer is used; in some cases growth is started on a nominally clean Si substrate, which, however, can easily exhibit small patches of silicon oxide. An organic layer on a clean Si surface was proven to break up before growth[12] most likely creating oxide patches on the surface. The In particles have to form in the early states of growth, like in the work here, as in most cases no intentional In particle formation was reported. In all cases it is reasonable to assume that the substrate is partially covered with a mask equivalent to the SiO_x layer we used, which immobilizes group III particles necessary for nanowire nucleation and at the same time provides openings ensuring epitaxial growth. For many investigations performed in this growth regime, no particle is found at the wire top after growth; this can be explained by the long cooling time under a group V flow, especially in MOVPE systems, which gives the particle enough time to form a crystalline material. For In−V growth at low substrate temperature (300−450 °C) (the second regime),[13,31,33−35] as extensively studied for InP, the use of a layer on the substrate surface seems less important, as the mobility of In on the surface is already considerably reduced and a layer is not required to prevent the formation of large In particles. It was shown that by intentional formation of In particles on the substrate prior to growth, achieved by deposition of In prior to growth, nanowires can be grown at these low temperatures. Here, after growth, the In particles are still observable, due to the low growth rate and shorter cooling times. The results of an extensive study of InP nanowire growth on InP(111)B show a loss of the In particle during/

DOI: 10.1021/nl1022699 | *Nano Lett.* **2010,** *10,* 4443–4449

after growth depending on V/III ratio and decomposition state of the used group V precursor.[13,42] In all cases In droplets seed the wire growth, but for higher growth temperatures a passivation layer on the surface is needed to stabilize small In droplets required for wire nucleation.

For the growth of Ga−V nanowires, ultrathin silicon oxide layers, thick SiO_2 layers with pitch holes, or lithographically patterned layers are used.[37,43] For GaAs growth the situation is actually more complicated, it has been shown that, depending on the V/III ratio, a transition between PAG to SAE is possible.[44] It is reasonable that with increasing electronegativity of the group III and group V elements, SAE becomes more favorable. For PAG an oxide layer with openings was present in all cases. It is thus quite conceivable that growth follows the same mechanism as described above, with a Ga particle substituting for the In. A Ga particle has even been found after growth,[37] for nanowires grown by molecular beam epitaxy. In this case, the growth rate is much smaller, and the cooling time under As flow is shorter than 1 min, so that the Ga particle does not have sufficient time to form GaAs. The fact, however, that even under those rather different growth conditions the same mechanism for wire formation has been found, namely, vapor−liquid−solid growth with a homoparticle stabilized by a mask layer, could indicate the universal character of the proposed mechanism.

Acknowledgment. The authors thank W. Seifert, K. A. Dick, and M. Cantoro for helpful discussions and K. Storm for providing image interpretation software. This work was carried out within the Nanometer Structure Consortium at Lund University (nmC@LU) and was supported by the Swedish Research Council (VR), the Swedish Foundation for Strategic Research (SSF) and the Knut and Alice Wallenberg Foundation, the EU Projects NODE (Contract No. 015783), SANDiE (Contract No. NMP4-CT-2004-500101), and AMONRA (Contract No. 214814), and by the FWF Vienna by the SFB project IRON (F2507-N08).

Supporting Information Available. Movie of in situ LEEM view during SiO_x covered substrate annealing. This material is available free of charge via the Internet at http://pubs.acs.org.

REFERENCES AND NOTES

(1) Caroff, P.; Wagner, J. B.; Dick, K. A.; Nilsson, H. A.; Jeppsson, M.; Deppert, K.; Samuelson, L.; Wallenberg, L. R.; Wernersson, L. *Small* **2008**, *4*, 878–882.
(2) Bjork, M. T.; Ohlsson, B. J.; Sass, T.; Persson, A. I.; Thelander, C.; Magnusson, M. H.; Deppert, K.; Wallenberg, L. R.; Samuelson, L. *Nano Lett.* **2002**, *2*, 87–89.
(3) Gudiksen, M. S.; Lauhon, L. J.; Wang, J.; Smith, D. C.; Lieber, C. M. *Nature* **2002**, *415*, 617–620.
(4) Dick, K. A. *Prog. Cryst. Growth Charact. Mater.* **2008**, *54*, 138–173.
(5) Li, Y.; Qian, F.; Xiang, J.; Lieber, C. M. *Mater. Today* **2006**, *9*, 18–27.
(6) Samuelson, L. *Mater. Today* **2003**, *6*, 22–31.
(7) Ikejiri, K.; Noborisaka, J.; Hara, S.; Motohisa, J.; Fukui, T. *J. Cryst. Growth* **2007**, *298*, 616–619.
(8) Tomioka, K.; Motohisa, J.; Hara, S.; Fukui, T. *Nano Lett.* **2008**, *8*, 3475–3480.
(9) Mohammad, S. N. *J. Vac. Sci. Technol. B: Microelectron. Nanometer Struct.—Process., Meas., Phenom.* **2008**, *26*, 1993–2007.
(10) Zhang, R.; Lifshitz, Y.; Lee, S. *Adv. Mater.* **2003**, *15*, 635–640.
(11) Wei, W.; Bao, X.; Soci, C.; Ding, Y.; Wang, Z.; Wang, D. *Nano Lett.* **2009**, *9*, 2926–2934.
(12) Mårtensson, T.; Wagner, J. B.; Hilner, E.; Mikkelsen, A.; Thelander, C.; Stangl, J.; Ohlsson, B. J.; Gustafsson, A.; Lundgren, E.; Samuelson, L.; Seifert, W. *Adv. Mater.* **2007**, *19*, 1801–1806.
(13) Woo, R. L.; Gao, L.; Goel, N.; Hudait, M. K.; Wang, K. L.; Kodambaka, S.; Hicks, R. F. *Nano Lett.* **2009**, *9*, 2207–2211.
(14) Xia, Y.; Yang, P.; Sun, Y.; Wu, Y.; Mayers, B.; Gates, B.; Yin, Y.; Kim, F.; Yan, H. *Adv. Mater.* **2003**, *15*, 353–389.
(15) Khayer, M. A.; Lake, R. K. *J. Appl. Phys.* **2010**, *107*, No. 014502.
(16) Thelander, C.; Fröberg, L. E.; Rehnstedt, C.; Samuelson, L.; Wernersson, L. *IEEE Electron Device Lett.* **2008**, *29*, 206–208.
(17) Wacaser, B. A.; Dick, K. A.; Johansson, J.; Borgström, M. T.; Deppert, K.; Samuelson, L. *Adv. Mater.* **2009**, *21*, 153–165.
(18) www.elmitec.de.
(19) Nyholm, R.; Andersen, J. N.; Johansson, U.; Jensen, B. N.; Lindau, I. *Nucl. Instrum. Methods Phys. Res., Sect. A* **2001**, *467−468*, 520–524.
(20) Park, C.; Jung, W.; Huang, Z.; Anderson, T. J. *J. Mater. Chem.* **2002**, *12*, 356–360.
(21) Zinke-Allmang, M.; Feldman, L. C.; Grabow, M. H. *Surf. Sci. Rep.* **1992**, *16*, 377–463.
(22) The growth mechanism of nanowires needs not be the same for all substrates in the first place. However, since the growth conditions and the obtained nanowire parameters are extremely similar in all cases, it is very unlikely that different mechanisms give virtually exactly the same result.
(23) Mandl, B.; Stangl, J.; Mårtensson, T.; Mikkelsen, A.; Eriksson, J.; Karlsson, L.; Bauer, G.; Samuelson, L.; Seifert, W. *Nano Lett.* **2006**, *6*, 1817–1821.
(24) Tersoff, J.; Jesson, D. E.; Tang, W. X. *Science* **2009**, *324*, 236–238.
(25) Hilner, E.; Zakharov, A. A.; Schulte, K.; Kratzer, P.; Andersen, J. N.; Lundgren, E.; Mikkelsen, A. *Nano Lett.* **2009**, *9*, 2710–2714.
(26) In experiments performed later, we found that the annealing step prior to growth has no influence.
(27) Larsen, C. A.; Buchan, N. I.; Stringfellow, G. B. *Appl. Phys. Lett.* **1988**, *52*, 480.
(28) Lee, J. H.; Wang, Z. M.; Kim, N. Y.; Salamo, G. J. *Nanotechnology* **2009**, *20*, 285602.
(29) Tomioka, K.; Mohan, P.; Noborisaka, J.; Hara, S.; Motohisa, J.; Fukui, T. *J. Cryst. Growth* **2007**, *298*, 644–647.
(30) Akabori, M.; Sladek, K.; Hardtdegen, H.; Schäpers, T.; Grützmacher, D. *J. Cryst. Growth* **2009**, *311*, 3813–3816.
(31) Dayeh, S. A.; Yu, E. T.; Wang, D. *Small* **2007**, *3*, 1683–1687.
(32) Cantoro, M.; Brammertz, G.; Richard, O.; Bender, H.; Clemente, F.; Leys, M.; Degroote, S.; Caymax, M.; Heyns, M.; Gendt, S. D. *J. Electrochem. Soc.* **2009**, *156*, H860–H868.
(33) Mattila, M.; Hakkarainen, T.; Lipsanen, H.; Jiang, H.; Kauppinen, E. I. *Appl. Phys. Lett.* **2006**, *89*, No. 063119−3.
(34) Gao, L.; Woo, R. L.; Liang, B.; Pozuelo, M.; Prikhodko, S.; Jackson, M.; Goel, N.; Hudait, M. K.; Huffaker, D. L.; Goorsky, M. S.; Kodambaka, S.; Hicks, R. F. *Nano Lett.* **2009**, *9*, 2223–2228.
(35) Mattila, M.; Hakkarainen, T.; Jiang, H.; Kauppinen, E. I.; Lipsanen, H. *Nanotechnology* **2007**, *18*, 155301.
(36) Colombo, C.; Spirkoska, D.; Frimmer, M.; Abstreiter, G.; Fontcuberta i Morral, A. *Phys. Rev. B* **2008**, *77*, 155326.
(37) Fontcuberta i Morral, A.; Colombo, C.; Abstreiter, G.; Arbiol, J.; Morante, J. R. *Appl. Phys. Lett.* **2008**, *92*, No. 063112.
(38) Fontcuberta i Morral, A.; Spirkoska, D.; Arbiol, J.; Heigoldt, M.; Morante, J. R.; Abstreiter, G. *Small* **2008**, *4*, 899–903.
(39) Jabeen, F.; Grillo, V.; Rubini, S.; Martelli, F. *Nanotechnology* **2008**, *19*, 275711.
(40) Plissard, S.; Dick, K. A.; Wallart, X.; Caroff, P. *Appl. Phys. Lett.* **2010**, *96*, 121901.
(41) Lugstein, A.; Andrews, A. M.; Steinmair, M.; Hyun, Y.; Bertagnolli, E.; Weil, M.; Pongratz, P.; Schramböck, M.; Roch, T.; Strasser, G. *Nanotechnology* **2007**, *18*, 355306.
(42) Li, S.; Larsen, C.; Buchan, N.; Stringfellow, G. *J. Electron. Mater.* **1989**, *18*, 457–464.
(43) Noborisaka, J.; Motohisa, J.; Fukui, T. *Appl. Phys. Lett.* **2005**, *86*, 213102.
(44) Spirkoska, D.; Colombo, C.; Heiss, M.; Abstreiter, G.; Fontcuberta i Morral, A. *J. Phys.: Condens. Matter* **2008**, *20*, 454225.

DOI: 10.1021/nl1022699 | *Nano Lett.* **2010,** *10,* 4443–4449